

Quantum-state engineering using enhanced tripartite interactions in atom-photon-phonon hybrid systems

Yaowu Guo(郭耀武), Jiaqiang Zhao(赵加强), Lianzhen Cao(曹连振), Yingde Li(李英德), and Hong-Yan Lu(路红艳)

Citation : Chin. Phys. B, 2025, 34 (**2**): 024203. DOI: 10.1088/1674-1056/ad9a5d
Journal homepage: http://cpb.iphy.ac.cn; http://iopscience.iop.org/cpb

What follows is a list of articles you may be interested in

Giant enhancement of negative friction by resonant coupling between localized surface phonon polaritons and graphene plasmonics

Kaipeng Liu(柳开鹏), Shuai Zhou(周帅), Shiwei Dai(戴士为), and Lixin Ge(葛力新)
Chin. Phys. B, 2025, 34 (**1**): 014202. DOI: 10.1088/1674-1056/ad886c

Enhanced mechanical squeezing in an optomechanical system via backward stimulated Brillouin scattering

Shan-Shan Chen(陈珊珊), Yi-Long Xie(谢亦龙), Jing-Jing Zhang(张京京), Na-Na Zhang(张娜娜), Yong-Rui Guo(郭永瑞), Huan Yang(杨桓), and Yong Ma(马勇)
Chin. Phys. B, 2025, 34 (**1**): 014201. DOI: 10.1088/1674-1056/ad8cc0

Presentation of the Berry-Tabor conjecture in Lévy plates

Chao Li(李超) and Guo-Lin Hou(侯国林)
Chin. Phys. B, 2024, 33 (**10**): 104204. DOI: 10.1088/1674-1056/ad21f2

Parallel generation of 31 tripartite entangled states based on optical frequency combs

Jing Zhang(张静), Yan-Fang Wang(王艳芳), Xiao-Yu Liu(刘晓宇), Rong-Guo Yang(杨荣国)
Chin. Phys. B, 2017, 26 (**12**): 124205. DOI: 10.1088/1674-1056/26/12/124205

Output three-mode entanglement via coherently prepared inverted Y-type atoms

Wang Fei (王飞), Qiu Jing (邱晶)
Chin. Phys. B, 2014, 23 (**4**): 044203. DOI: 10.1088/1674-1056/23/4/044203

Quantum-state engineering using enhanced tripartite interactions in atom–photon–phonon hybrid systems

Yaowu Guo(郭耀武)[1,2,†], Jiaqiang Zhao(赵加强)[1], Lianzhen Cao(曹连振)[1], Yingde Li(李英德)[1], and Hong-Yan Lu(路红艳)[3]

[1] *Department of Physics and Electronic Information, Weifang University, Weifang* 261061, *China*
[2] *State Key Laboratory of Surface Physics and Laboratory of Advanced Materials, Department of Physics, Fudan University, Shanghai* 200433, *China*
[3] *School of Physics and Physical Engineering, Qufu Normal University, Qufu* 273165, *China*

(Received 2 September 2024; revised manuscript received 30 November 2024; accepted manuscript online 4 December 2024)

We introduce a hybrid cavity optomechanical model capable of generating significant genuine tripartite interactions and entanglement among coherent degrees of freedom. However, realizing and controlling such tripartite interactions and their entanglement pose crucial challenges that remain largely unexplored. In this work, we predict a tripartite coupling mechanism within a hybrid quantum system consisting of a vibrating mechanical oscillator, a two-level atom and a single-frequency cavity field. We specifically propose a mechanism for tripartite and cross-Kerr nonlinear coupling through displacement and squeezing transformations. By adjusting the optical amplitude of the pump light, we can effectively enhance these nonlinear couplings, facilitating the manipulation of entangled and squeezed states. The resulting tripartite genuine entanglement exhibits distinct evolutionary characteristics. Notably, when the pump light amplitude is large, the tripartite entanglement persists for longer time. Additionally, the phonon displays characteristics of both cooling and squeezing. Our study presents a pathway for exploring and exploiting controllable multipartite entanglement, as well as achieving phonon cooling and squeezing with the assistance of a mesoscopic harmonic oscillator. This work underscores the innovative potential of our model in advancing the field of optomechanics and quantum entanglement.

Keywords: cross-Kerr nonlinear coupling, tripartite coupling, tripartite entanglement

PACS: 42.50.Lc, 42.50.Pq, 62.25.Jk

DOI: 10.1088/1674-1056/ad9a5d **CSTR:** 32038.14.CPB.ad9a5d

1. Introduction

Cavity optomechanics (COM) traditionally focuses on the pairwise interaction between optical fields and macroscopic mechanical motion through radiation pressure.[1–7] However, explorations extending beyond these pairwise interactions have garnered significant interest.[8] Hybrid cavity optomechanical systems, in particular, can integrate disparate degrees of freedom to achieve novel functions, such as generating multi-particle entanglement, which is unattainable with individual degrees of freedom.[9,10] Meanwhile, cavity quantum electrodynamics (QED) has delved into resonant light–matter coupling between confined photon modes and atom-like electronic excitations.[11,12]

With advances in nanotechnology, hybrid systems combining COM and cavity QED have become feasible. These systems enable the simultaneous realization of tripartite and cross-Kerr nonlinear interactions, which remain largely unexplored. Recently, novel systems with rich hybrid structures have attracted considerable attention. Superconducting circuits[13,14] and hybrid spin–mechanical systems[15] have been studied for their potential to enhance various interactions. Systems incorporating two-level atoms also show strong optomechanical coupling.[16–20] Additionally, COM systems coupled to atomic ensembles have been investigated.[21–25]

Despite these studies, a genuine tripartite coupling regime has not been achieved. A recent theoretical scheme proposed tripartite coupling in spin–magnon–mechanical hybrid systems.[26] While pairwise interactions among atoms, photons and phonons have been presented,[27] the implementation of tripartite coupling among them remains rare. Therefore, hybrid systems combining COM and cavity QED are expected to realize such tripartite coupling and further form cross-Kerr nonlinear coupling.[28–31] Our work aims to address this gap by proposing a novel hybrid system that achieves and regulates tripartite coupling, contributing to the advancement of multipartite entanglement and quantum control.

In this article, we present an experimentally feasible hybrid quantum model, illustrated in Fig. 1(a), designed to generate tripartite coupling. The model consists of a Fabry–Pérot cavity, a movable mechanical resonator and a two-level atom. The resonator is positioned at the node (or antinode) of the intracavity optical mode, enabling quadratic coupling to the single optical mode.[32,33,47] As the two-level atom interacts with the single-mode photon, it harmoniously oscillates with the resonator, transforming the pairwise interaction between the photon and atom into a tripartite interaction. A quantized

[†]Corresponding author. E-mail: guoyaowu@wfu.edu.cn

© 2025 Chinese Physical Society and IOP Publishing Ltd. All rights, including for text and data mining, AI training, and similar technologies, are reserved.

description reveals the participation of the phonon in this interaction.

Our hybrid quantum model, characterized by genuine atom–photon–phonon coupling, plays a distinctive role in quantum information processing. Firstly, when the intensity of the pump light field is strong, it effectively modulates the strength of the tripartite coupling, making the amplitude of the pump light a crucial and experimentally adjustable parameter for the hybrid system.[36] Increasing the amplitude of the pump light enhances the strength of both tripartite and cross-Kerr nonlinear couplings, contributing to phonon cooling and squeezing. Given the distinct characteristics of pairwise and tripartite entanglement,[37–42] we will analyze the time-dependent behavior of tripartite entanglement. These behaviors can be modulated through the pumping field and field decay factors, exhibiting different evolutionary patterns as decay factors increase. Secondly, based on strong and genuine tripartite interactions at the single quantum level, the framework of multi-particle entanglement offers a powerful tool for quantum information processing applications.[41,42] Our model thus provides a novel platform for exploring and harnessing the potential of tripartite coupling in quantum systems.

2. The model

As depicted in Fig. 1(a), a mechanical oscillator, carrying a two-level atom, is positioned at the node of the intracavity field.[43] This setup encompasses three degrees of freedom: the single two-level atom ($\hat{\sigma}_i$), the photon mode ($\hat{c}$) and the mechanical mode ($\hat{b}$). The atom operators are defined by the Pauli operators $\hat{\sigma}_i$ (with $i = x, y, z$) in the two-level energy basis $\{|g\rangle, |e\rangle\}$. Within the hybrid cavity, we model the interaction between photons and the two-level atom using the Jaynes–Cummings (JC) form Ref. [44] and a quadratic optomechanical coupling between phonons ($\hat{b}$) and photons ($\hat{c}$). As the two-level atom undergoes simple harmonic vibration, phonons participate in the cavity QED interaction, leading to the formation of atom–photon–phonon coupling, as illustrated in Fig. 1(b).The total Hamiltonian of the system, with $\hbar = 1$, can be expressed as follows:[45]

$$\hat{H}_{\text{total}} = \hat{H}_{\text{T0}} + \hat{H}_{\text{Om}} + \hat{H}_{\text{Tr}} + \hat{H}_{\text{Dr}}, \tag{1}$$

with

$$\hat{H}_{\text{T0}} = \omega_c \hat{c}^\dagger \hat{c} + (\omega_a/2)\hat{\sigma}_z + \omega_b \hat{b}^\dagger \hat{b}, \tag{2}$$

$$\hat{H}_{\text{Om}} = g\hat{c}^\dagger \hat{c}(\hat{b}^\dagger + \hat{b})^2, \tag{3}$$

$$\hat{H}_{\text{Tr}} = \lambda^{\text{tr}}(\hat{\sigma}_+ \hat{b}^\dagger \hat{c} + \hat{\sigma}_- \hat{b}\hat{c}^\dagger + \hat{b}\hat{\sigma}_+ \hat{c} + \hat{b}^\dagger \hat{\sigma}_- \hat{c}^\dagger), \tag{4}$$

$$\hat{H}_{\text{Dr}} = \varepsilon_c(\hat{c}e^{i\omega_L t} + \hat{c}^\dagger e^{-i\omega_L t}), \tag{5}$$

where $\hat{c}$ ($\hat{c}^\dagger$) and $\hat{b}$ ($\hat{b}^\dagger$) denote the annihilation (creation) operators of the cavity (with resonant frequency ω_c) and mechanical modes (with resonant frequency ω_b), g characterizes the quadratic optomechanical coupling and H_{T0} describes the Hamiltonian of the cavity field, the single atom and the phonons respectively. H_{Tr} describes the tripartite coupling and λ^{tr} is the atom–photon–phonon coupling strength. $\hat{H}_{\text{Dr}}$ is the pumping field of the cavity mode, where ε_c is a slowly varying amplitude related to the input laser power P by $\varepsilon_c = \sqrt{P\gamma_c/(\hbar\omega_L)}$. γ_c is the photon decay rate in the cavity field.

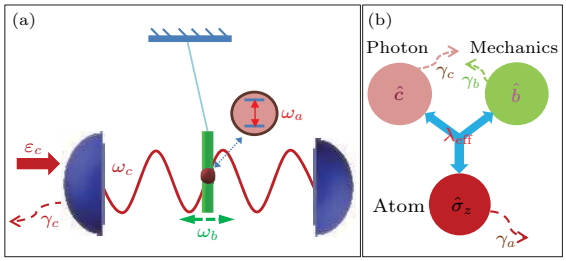


Fig. 1. (a) Proposal schematic: A mechanical oscillator vibrates harmonically at frequency ω_b within a single-mode optical cavity (ω_c). A two-level atom (ω_a) is embedded in the oscillator. Quadratic optomechanical coupling links the oscillator and the optical mode, while cavity QED interaction connects the optical mode and the atom. (b) Physical model schematic: The two-level atom (red circle), phonon mode (cyan ellipse), and photon mode (green circle) are coupled simultaneously. Photonic driving (blue wavy arrow) enhances the coupling rate to λ_{eff} (blue trichotomous arrow).

In the subsequent analysis, we delve into the generation of tripartite coupling within the hybrid optomechanical system. Within the confines of the hybrid cavity QED system, the electric field operator is given by $\hat{\boldsymbol{E}}(z,t) = \boldsymbol{e}_x\sqrt{\hbar\omega_c/(\varepsilon_0 V)}\sin(k_c z)(\hat{c} + \hat{c}^\dagger)$. Here, a monochromatic optical mode engages with a two-level atom, and the corresponding Hamiltonian is formulated as follows:[46]

$$\hat{H}_{\text{cavity QED}} = -\hat{\boldsymbol{d}} \cdot \hat{\boldsymbol{E}}_{z,t}, \tag{6}$$

where $\hat{\boldsymbol{d}}$ is the atomic dipole operator $\hat{\boldsymbol{d}} = d(\hat{\sigma}_+ + \hat{\sigma}_-)$. From Eq. (6), we obtain the quantized Hamiltonian

$$\hat{H}_{\text{Tr}}(z) = \lambda k_c \hat{z}(\hat{\sigma}_+ + \hat{\sigma}_-)(\hat{c} + \hat{c}^\dagger), \tag{7}$$

where λ is the atom–field coupling constant. In the aforementioned equation, the two-level atom produces harmonic vibrations and is positioned at the nodes of the optical standing wave. Consequently, the electric dipole coupling becomes position-dependent,[45] approximated as $\sin(k_c z) \approx k_c z$. The quantized displacement can be expressed as $\hat{z} = z_0(\hat{b} + \hat{b}^\dagger)$, where $\hat{b}$ is the oscillator operator and $z_0 = \sqrt{\hbar/2m_{\text{eff}}\omega_b}$ denotes the zero-point fluctuation. By applying the rotating wave approximation, we can easily derive Eq. (4) from Eq. (7) with the effective tripartite coupling rate $\lambda^{\text{tr}} = \lambda k_c z_0$, $\eta = k_c z_0$, and $\lambda^{\text{tr}} = \lambda\eta$. k_c denotes the magnitude of the wave vector of the optical field, while m_{eff} represents the effective mass of a two-level atom embedded in a simple harmonic oscillator. This effective mass is determined by the combined mass distribution of the oscillator and the atom. By vertically adjusting the atom's position, as depicted in Fig. 1(a), we can modify

$m_{\rm eff}$. In experiments, both $m_{\rm eff}$ of the atomic harmonic vibration and k_c of the light field can be adjusted simultaneously to precisely control the strength of the tripartite coupling $\lambda^{\rm tr}$. These two externally adjustable parameters provide a practical experimental method to effectively manage and enhance the tripartite interaction.

With the aid of strong and adjustable driving fields, we can significantly increase both optomechanical and tripartite couplings.[47] To better illustrate the impact of these driving fields, the Hamiltonian can be transformed into a more suitable physical framework. In the interaction picture at frequency $\omega_{\rm L}$, the driving field component of the optical field can be removed by converting the Hamiltonian into a displacement form using $\hat{H}_{\rm D} = D^{\dagger}(\alpha)\hat{H}_{\rm total}D(\alpha)$. Here, the displacement operator $D(\alpha)$ is defined by $D^{\dagger}(\alpha)\hat{c}D(\alpha) = \hat{c}+\alpha$, and it can be written as

$$\begin{aligned}\hat{H}_{\rm D} = {}& \Delta_c\hat{c}^{\dagger}\hat{c} + (\widetilde{\omega}_a/2)\hat{\sigma}_z + \omega_b\hat{b}^{\dagger}\hat{b} + \hat{H}_{\rm sp} \\ & - g[\hat{c}^{\dagger}\hat{c} + \alpha(\hat{c}^{\dagger}+\hat{c}) + \alpha^2](\hat{b}^{\dagger}+\hat{b})^2 \\ & + \lambda^{\rm tr}(\hat{\sigma}_+\hat{b}^{\dagger}\hat{c} + \hat{\sigma}_-\hat{b}\hat{c}^{\dagger} + \hat{\sigma}_+\hat{b}\hat{c} + \hat{\sigma}\hat{b}^{\dagger}\hat{c}^{\dagger}), \end{aligned} \tag{8}$$

where the detunings are defined as $\Delta_c = \omega_c - \omega_{\rm L}$, $\widetilde{\omega}_a = \omega_a - \omega_{\rm L}$. Without the loss of generality, α is taken as a real number, specifically $\alpha = -\varepsilon_c/\Delta_c$. The equation presented above has ignored constant terms and incorporates the spin–phonon interaction $\hat{H}_{\rm sp} = \lambda^{\alpha}(\hat{\sigma}_+\hat{b} + \hat{\sigma}\hat{b}^{\dagger})$, where the coupling rate λ^{α} is given by $\lambda^{\alpha} = \lambda^{\rm tr}\alpha$.

3. Tripartite coupling enhanced by the driving field

In the Hamiltonian, Eq (8), the quadratic term of the mechanical mode can be diagonalized through the application of the squeezing transformation. This is achieved by $\hat{H}_{\rm eff} = S(r_\alpha)\hat{H}_{\rm D}S^{\dagger}(r_\alpha)$, where $S(r_\alpha)$ represents the squeezing operator defined as $S(r_\alpha) = \exp(r_\alpha(\hat{b}^2 - \hat{b}^{\dagger 2}))$. The squeezing amplitude r_α is defined as $r_\alpha = -\frac{1}{4}\ln(1-4g\alpha^2/\omega_b)$. Within this squeezing frame, the effective system Hamiltonian can be expressed as follows:[48,49]

$$\begin{aligned}\hat{H}_{\rm eff} = {}& \Delta_c\hat{c}^{\dagger}\hat{c} + (\widetilde{\omega}_a/2)\hat{\sigma}_z + \omega_b^{\alpha}\hat{b}^{\dagger}\hat{b} - g_\alpha(\hat{c}\hat{b}^{\dagger 2} + \hat{c}^{\dagger}\hat{b}^2) \\ & - 2g_{\rm K}\hat{c}^{\dagger}\hat{c}\hat{b}^{\dagger}\hat{b} + \lambda_{\rm eff}^{\rm tr}(\hat{\sigma}_+\hat{b}^{\dagger}\hat{c} + \hat{\sigma}_-\hat{b}\hat{c}^{\dagger}) + \hat{H}'_{\rm sp}, \end{aligned} \tag{9}$$

where $\omega_b^{\alpha} = \omega_b {\rm e}^{-2r_\alpha}$, $g_{\rm K} = g{\rm e}^{2r_\alpha}$ and $g_\alpha = g_{\rm K}\alpha$, with $g_{\rm K}$ denoting the cross-Kerr nonlinear coefficient. The tripartite effective coupling rate $\lambda_{\rm eff}^{\rm tr}$ is given by $\lambda^{\rm tr}{\rm e}^{r_\alpha}$, which can be enhanced and tuned by controlling ε_c. Additionally, $\hat{H}'_{\rm sp} = \lambda_{ab}^{\alpha}(\hat{\sigma}^+\hat{b} + \hat{\sigma}\hat{b}^{\dagger})$ with $\lambda_{ab}^{\alpha} = \lambda_\alpha {\rm e}^{r_\alpha}$. The atom has two states: a ground state $|g\rangle$ and an excited state $|e\rangle$. The particle numbers of the photon and phonon are labeled by $\{n,m\}$. Under blue detuning $\Delta_c \sim \omega_a + \omega_b^{\alpha}$ and the rotating wave approximation, the Hamiltonian permits interactions $\{\hat{c}\hat{b}^{\dagger 2}, \hat{b}\hat{\sigma}^+, \hat{c}\hat{b}^{\dagger}\hat{\sigma}^+\} + {\rm H.c.}$ in Eq. (9), corresponding to transitions $\sum_{n,m}\{|g,n,m\rangle \leftrightarrow |g,n-1,m+2\rangle \leftrightarrow |e,n-1,m+1\rangle \leftrightarrow |e,n,m-1\rangle\}$. These transitions describe the annihilation and excitation of photons, phonons and atomic spins.

The dynamics of the open system are governed by the quantum master equation (accounting for field decays)

$$\frac{{\rm d}\hat{\rho}}{{\rm d}t} = -{\rm i}[\hat{H}_{\rm eff},\hat{\rho}] + \gamma_c L[\hat{c}]\hat{\rho} + \gamma_a L[\hat{\sigma}^-]\hat{\rho} + \gamma_b L[\hat{b}]\hat{\rho}, \tag{10}$$

where $\hat{\rho}$ is the density operator and $\gamma_{c,b,a}$ are the damping rates. The Lindblad dissipative terms, $\forall\hat{c}, L[\hat{c}]\rho = \hat{c}\rho\hat{c}^{\dagger} - \frac{1}{2}(\hat{c}^{\dagger}\hat{c}\rho + \rho\hat{c}^{\dagger}\hat{c})$, represent dissipations. For simplicity, we assume equal decay rates for phonons and photons, $\gamma_c = \gamma_b = \gamma$.

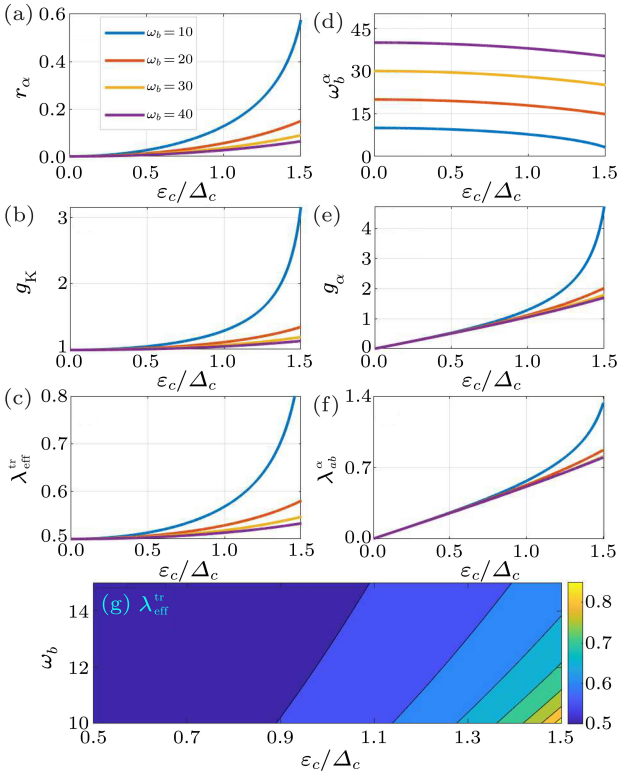


Fig. 2. The dependence of the squeezing parameter and the coupling parameter on the ratio ε_c/Δ_c of the pumping field of the cavity mode with different $\omega_b = 10, 20, 30, 40$. (a) The squeezing parameter r_α versus the amplitude ε_c/Δ_c of the pumping field, (b)–(f) ω_b^{α}, g_α, $g_{\rm K}$, λ_{ab}^{α} and $\lambda_{\rm eff}^{\rm tr}$ versus the amplitude ratio ε_c/Δ_c with different ω_b, respectively. (g) Contour map of tripartite coupling enhancement $\lambda_{\rm eff}^{\rm tr}$ versus the ratio ε_c/Δ_c and ω_b. Here $\omega_a = \omega_b = 10g$, $\Delta_c = 20g$ and $2\lambda^{\rm tr} = g = 1$.

To quantify the simultaneous enhancement of various couplings (tripartite, bipartite and cross-Kerr nonlinear), we explore the dependence of the squeezing amplitude r_α and model coupling parameters on the pumping field amplitude ε_c, as depicted in Fig. 2. The squeezing parameter, tripartite coupling strength $\lambda_{\rm eff}^{\rm tr}$ and cross-Kerr coupling $g_{\rm K}$ exhibit exponential enhancement due to amplified phonon fluctuations, which increase with ε_c [Figs. 2(a)–2(c)]. Conversely, the effective phonon frequency ω_b^{α} decreases gradually [Fig. 2(d)]. Both the quadratic optomechanical coupling g_α and the spin–phonon coupling λ_{ab}^{α} show a faster enhancement trend than typical exponential growth [Figs. 2(e) and 2(f)]. Notably, $\lambda_{\rm eff}^{\rm tr}$

demonstrates further exponential enhancement, inversely proportional to ω_b [Fig. 2(g)]. In summary, by adjusting the driving field strength ε_c within the framework of phonon squeezing we can simultaneously realize and regulate the hybrid quantum system, enhancing both tripartite and bipartite interactions.

4. Dynamics of the cooling processes in a hybrid cavity system

When tripartite and bipartite couplings coexist, exploring the evolution of quasi-particle occupancy under ideal conditions becomes crucial. Numerical solutions for the occupancy dynamics of the two-level atom, photon and phonon, as depicted in Fig. 3, illuminate the cooling processes within the hybrid system. Figures 3(a) and 3(b) display the time evolution of photon and phonon occupancies, respectively, for various decay rates ($\gamma = \gamma_c = \gamma_b$). The asymptotic behavior of photon occupancy reveals a convergence to a finite steady-state value under $\varepsilon_c = 15$ [Fig. 3(a)], whereas phonon occupancy eventually diminishes to zero, indicating complete phonon cooling [Fig. 3(b)]. The inset underscores the universality of the atomic population cooling process over time. Notably, artificially enhancing the decay coefficients ($\gamma = \gamma_c = \gamma_b$) can optimize the rate of phonon cooling.

Figures 3(c) and 3(d) present the time evolution of photon and phonon occupancies for different strengths of the pumping field (ε_c). When ε_c is below a threshold value of 10, photon occupancy ultimately vanishes, realizing photon cooling [Fig. 3(c)]. Conversely, as shown in the inset, phonon cooling remains relatively insensitive to the magnitude of ε_c. Under a strong driving field, the atomic population evolves from a finite value (> -0.5) over time, while in a weak field it remains in the ground state ($= -0.5$) without temporal change. It is worth mentioning that the initial states for the system's evolution are derived from the ground states of the closed system at varying ε_c [Fig. 3(d)].

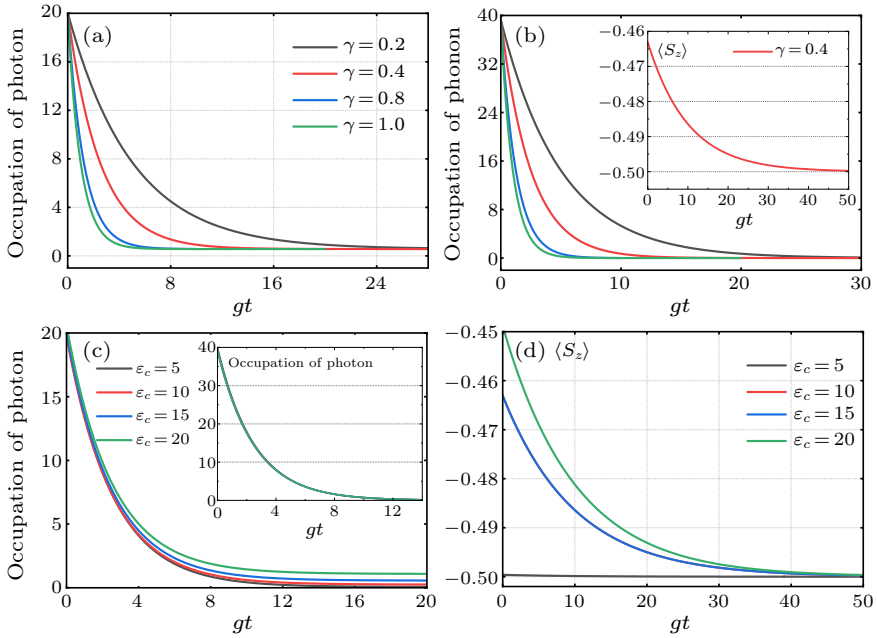


Fig. 3. Quantum asymptotic dynamics in cooling processes. (a) Time evolution of the steady-state photon number with different decays $\gamma = \gamma_c = \gamma_b$, $\gamma_a = 0.1$, and (b) the mechanical phonon evolution. The inset shows universal time evolution of the atomic population for different decay parameters. (c) The dependence of time evolution of the photon number on the strength ε_c of the pumping field of the cavity mode with different $\varepsilon_c = 5$, 10, 15, 20. The inset shows universal time evolution of the phonon number. (d) The time evolution of the atomic population with different strengths ε_c of the pumping field. Here $\lambda^{\rm tr} = g = 1$ and $\gamma_a = 0.1$. Other parameters are shown in Fig. 2.

5. Applications of the tripartite coupling system

For a novel hybrid system featuring multiple types of couplings, tripartite entanglement emerges as a crucial physical parameter.[50] We assess the temporal dynamics of tripartite entanglement under varying driving field strengths ε_c and decay factors γ. The tripartite negativity provides a quantitative measure of the full tripartite entanglement of these states. Specifically, we define the genuine tripartite negativity of a state ρ as $N = (N_{\rm A-BC} N_{\rm B-AC} N_{\rm C-AB})^{1/3}$,[51] where the bipartite negativities are given by $N_{I-JK} = -2\sum_i \sigma_i(\rho_{\rm TI})$. Here, $\sigma_i(\rho_{\rm TI})$ represents the negative eigenvalues of $\rho_{\rm TI}$, and the partial transpose of ρ is defined as $\langle i_I, j_{JK} \mid \rho_{\rm TI} \mid k_I, l_{JK} \rangle = \langle k_I, j_{JK} \mid \rho \mid i_I, l_{JK} \rangle$ with respect to subsystem I (I = A, B, C) and JK = BC, AC, AB.

The evolution of the hybrid system starts from the ground state of the Hamiltonian in Eq. (9). Figure 4(a) illustrates the evolution of genuine tripartite entanglement under different driving fields $\varepsilon_c = 5$, 10, 15, 20 with a fixed decay factor $\gamma = 0.4$. It is evident that stronger driving field strengths lead to more robust and prolonged entanglement over time.

Clearly, enhancing the coupling strength of the system facilitates the maintenance of tripartite entanglement. Similarly, Fig. 4(b) demonstrates that the decay of tripartite entanglement accelerates with increasing decay factors $\gamma = 0.2$, 0.4, 0.8, 1. The stronger the decay factor, the faster the entanglement decays. Genuine tripartite entanglement is a valuable quantum information resource with numerous potential applications in quantum information processing[52–57] and quantum many-body physics.[58–62]

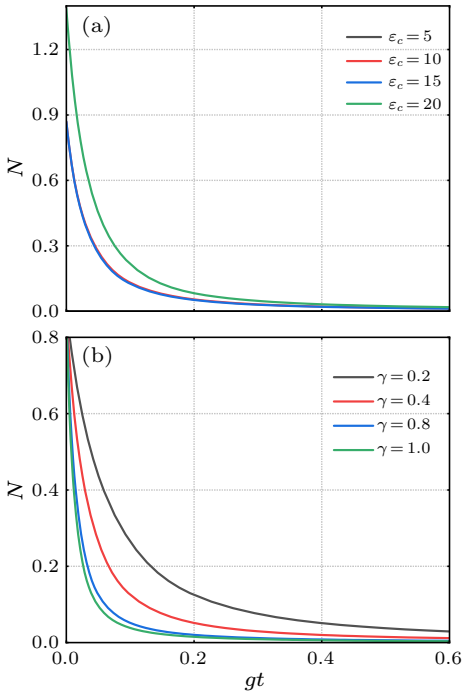


Fig. 4. The tripartite entanglement dynamics with different decays γ and strengths ε_c of the pumping field. (a) The dependence of the tripartite entanglement on the ε_c of the pumping field of the cavity mode with $\gamma = 0.4$. (b) The time evolution of three-body entanglement with different decay factors $\gamma = 0.2$, 0.4, 0.8, 1 and $\varepsilon_c = 15$. Here $\lambda^{\rm tr} = g = 1$, $\gamma_a = 0.1$. Other parameters are shown in Fig. 2.

Considering the quadratic term of the mechanical mode, we explore the quantum squeezing of mechanical phonons, a typical quantum effect and important resource for various applications.[63–66] We now analyze how the driving field and dissipation affect the squeezing properties of the oscillator. The squeezing of the oscillator can be assessed through the variances of its quadrature operators $X_+ = S(r_\alpha)(b^\dagger + b)S^\dagger(r_\alpha)$ and $X_- = S(r_\alpha)[\mathrm{i}(b^\dagger - b)]S^\dagger(r_\alpha)$, as detailed in Refs. [67,68],

$$\langle \Delta X_\pm^2 \rangle(t) = [1 + 2\langle b^\dagger b\rangle \pm (\langle b^2\rangle + \langle b^{\dagger 2}\rangle) \mp (\langle b^\dagger\rangle \pm \langle b\rangle)^2]\mathrm{e}^{\pm 2r_\alpha}. \tag{11}$$

Thus, mechanical phonon squeezing occurs when the variances fulfill the condition $\langle \Delta X_+^2\rangle < 1$ or $\langle \Delta X_-^2\rangle < 1$. Specifically, steady squeezing of the oscillator is observed solely in $\langle \Delta X_-^2\rangle(t)$. As depicted in Fig. 5(a), mechanical phonon squeezing, represented by $\langle \Delta X_-^2\rangle$, can be effectively modulated. An increase in the decay factor γ leads to the onset of phonon squeezing (indicated by values below the solid black line of 1), with a more rapid entry into the squeezing state and sustained squeezing over time. For a fixed decay factor, $\gamma = 0.4$, as the pumping field strength ε_c increases (5, 10, 15, 20), the phonon enters the squeezed state more swiftly and achieves better optimization, as illustrated in Fig. 5(b). Through the discussion of the above two applications, it can be found that the pumping field strength ε_c enhances both tripartite entanglement and phonon squeezing characteristics. Conversely, while the decay factor γ causes entanglement performance to decline over time it augments squeezing performance. Consequently, within our system, adjustable parameters ε_c and γ enable us to effectively achieve controllable tripartite entanglement and phonon squeezing at the single quantum level. This underscores the innovative aspect of our approach, facilitating precise control over these quantum phenomena through experimentally accessible means.

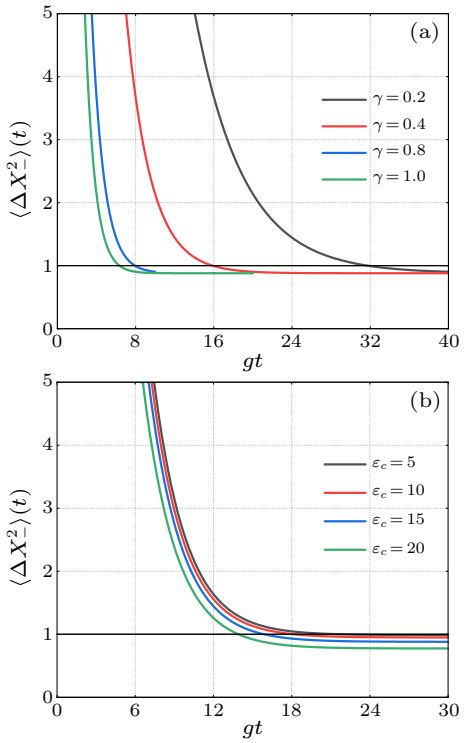


Fig. 5. The time evolution of the squeezing $\langle \Delta X_-^2\rangle$ of the mechanical phonon with different pump field strengths and decay factors. The dependence of time evolution of the squeezing on different decay factors $\gamma = 0.2$, 0.4, 0.8, 1, is shown in (a). (b) The dependence of time evolution of the squeezing on the strength ε_c of the pumping field of the cavity mode with different $\varepsilon_c = 5$, 10, 15, 20. Here $\lambda^{\rm tr} = g = 1$ and $\gamma_a = 0.1$. Other parameters are shown in Fig. 2.

6. The feasibility of the scheme in the experiment

In addition to the experimental scheme mentioned above, various hybrid optomechanical setups, besides the membrane-in-middle cavity system, such as cavity-levitated nanospheres and atom-chip-based cavity optomechanics, have demonstrated feasible quadratic coupling between the cavity mode

and mechanical oscillator.[69,70] To align our theoretical framework with experimental feasibility and operability, we aim to adopt parameters that mirror those used in actual experimental setups, such as those outlined by Thompson *et al.*[71] Typically, the mechanical frequency is set at $\omega/2\pi = 8.4\times 10^5$ Hz, with a mechanical decay constant of $\gamma_b = 0.75$ Hz. A key challenge lies in realizing the quadratic optomechanical coupling. Recent advances have significantly enhanced this experimentally accessible coupling strength. For the coupling strength $g = \frac{1}{2}\partial^2\omega_c/\partial z^2 z_0^2$ (z_0 being the mechanical zero-point fluctuation), the value of $\partial^2\omega_c/\partial z^2(0)$ sees a substantial increase from approximately 30 MHz/nm^2[73] to 20 GHz/nm^2[74] when using a fiber cavity with a smaller mode size. With $z_0 \sim 5$ pm, as suggested in Ref. [72], the coupling strength g can reach several kilohertz. Furthermore, a quadratic coupling of $g \sim 2\pi\times 0.7$ MHz has been theoretically estimated in a near-field optomechanical system.[75] Incorporating a nonlinear medium can further enhance g, potentially leading to a pronounced phonon blockade effect.[76]

7. Conclusion

In this paper, we propose an experimentally feasible scheme to simultaneously achieve both tripartite and cross-Kerr nonlinear couplings in the same quantum hybrid cavity system. We show that the strengths of the tripartite coupling and the cross-Kerr coupling can increase exponentially as the pumping field strength increases. The evolutionary dynamics of the cooling processes in the hybrid cavity system will be modulated via the pumping field strength (ε_c) and the decay factor (γ). We also discuss the dynamics of true tripartite entanglements and reveal the dependence of entanglement evolution on ε_c and γ. The entanglement duration and depth among the photon, the atom and the phonon can be significantly improved by increasing ε_c. Meanwhile robust mechanical squeezing can also be generated. We further show the conditions of realization for the mechanical phonon squeezing state. Finally, we come to the conclusion that, based on atom–photon–phonon tripartite coupling, the tripartite entangled state and the mechanical phonon squeezing state can be effectively realized through an experimentally adjustable driving field strength and the decay factor, which has potential applications in quantum technologies. In the future, this will also be a very advantageous platform for the study of quantum many-body interactions with strong feasibility.[77]

Appendix A: Derivation of the effective tripartite coupling in the system Hamiltonian

In this appendix, we first present more details about the Hamiltonian of the hybrid optomechanical system, and the generation of the tripartite coupling in hybrid optomechanical system will be derived in detail. We know the operator form of the electric field of the radiation field is denoted by $\hat{E}(z,t) = \boldsymbol{e}_x\sqrt{\hbar\omega_c/(\varepsilon_0 V)}\sin(k_c z))(\hat{c}+\hat{c}^\dagger)$. The interaction of a radiation field $\boldsymbol{E}$ with a two-level atom can be described by the following Hamiltonian in the dipole approximation:

$$\begin{aligned}\hat{H}_{\text{cavity QED}} &= -\boldsymbol{d}\cdot\boldsymbol{E}_{z,t}\\ &= -\boldsymbol{d}\cdot\boldsymbol{e}_x\sqrt{\hbar\omega_c/(\varepsilon_0 V)}\sin(k_c z))(\hat{c}+\hat{c}^\dagger)\\ &= -d(\hat{\sigma}_+ + \hat{\sigma}_-)\sqrt{\hbar\omega_c/(\varepsilon_0 V)}\sin(k_c z))(\hat{c}+\hat{c}^\dagger)\\ &= -d\sqrt{\hbar\omega_c/(\varepsilon_0 V)}\sin(k_c z)(\hat{\sigma}_+ + \hat{\sigma}_-)(\hat{c}+\hat{c}^\dagger),\end{aligned} \tag{A1}$$

with simple harmonic oscillation of the mechanical resonator carrying the two-level atom, and the mechanical oscillator vibrates near the equilibrium position, so $\sin(k_c z)\approx k_c z$ and the operator form of the oscillator coordinate z is $\hat{z} = z_0(\hat{b}+\hat{b}^\dagger)$ with $z_0 = \sqrt{\hbar/2m_{\text{eff}}\omega_b}$, and take it into the above formula and $\hat{H}_{\text{cavity QED}}$ becomes

$$\begin{aligned}\hat{H}_{\text{cavity QED}} &\approx -d\sqrt{\hbar\omega_c/(\varepsilon_0 V)}k_c\hat{z}(\hat{\sigma}_+ + \hat{\sigma}_-)(\hat{c}+\hat{c}^\dagger)\\ &= -d\sqrt{\hbar\omega_c/(\varepsilon_0 V)}k_c z_0(\hat{b}+\hat{b}^\dagger)(\hat{\sigma}_+ + \hat{\sigma}_-)(\hat{c}+\hat{c}^\dagger),\end{aligned} \tag{A2}$$

with $\lambda = -d\sqrt{\hbar\omega_c/(\varepsilon_0 V)}$, and $\eta = k_c z_0$.

$$\begin{aligned}\hat{H}_{\text{cavity QED}} &= \lambda\eta(\hat{b}+\hat{b}^\dagger)(\hat{\sigma}_+ + \hat{\sigma}_-)(\hat{c}+\hat{c}^\dagger)\\ &= \lambda\eta(\hat{b}\hat{\sigma}_+\hat{c} + \hat{b}\hat{\sigma}_+\hat{c}^\dagger + \hat{b}\hat{\sigma}_-\hat{c} + \hat{b}\hat{\sigma}_-\hat{c}^\dagger + \hat{b}^\dagger\hat{\sigma}_+\hat{c}\\ &\quad + \hat{b}^\dagger\hat{\sigma}_+\hat{c}^\dagger + \hat{b}^\dagger\hat{\sigma}_-\hat{c} + \hat{b}^\dagger\hat{\sigma}_-\hat{c}^\dagger).\end{aligned} \tag{A3}$$

Appendix B: The effective tripartite coupling of the system Hamiltonian

Let us take the resonance condition $\omega_c = 2\omega_b$, and the rotational wave approximation,

$$\hat{H}_{\text{Tr}} = \lambda^{\text{tr}}(\hat{b}\hat{\sigma}_+\hat{c} + \hat{b}\hat{\sigma}_-\hat{c}^\dagger + \hat{b}^\dagger\hat{\sigma}_+\hat{c} + \hat{b}^\dagger\hat{\sigma}_-\hat{c}^\dagger). \tag{B1}$$

This is just Eq. (4) and $\lambda^{\text{tr}} = \lambda k_c z_0$ is Eq. (8) in the main text.

Acknowledgements

This work was supported by the National Natural Science Foundation of China (Grant No. 12074213), the Natural Science Foundation of Shandong Province (Grant No. ZR2021MA078), and the Research Project of the National Key Laboratory (Grant No. KF2020_04).

References

[1] Aspelmeyer M, Kippenberg T J and Marquardt F 2014 *Rev. Mod. Phys.* **86** 1391
[2] Aspelmeyer M, Meystre P and Schwab K 2012 *Phys. Today* **65** 29
[3] Meystre P 2013 *Ann. Phys. (Berlin)* **525** 215
[4] Marquardt F and Girvin S M 2009 *Physics* **2** 40
[5] Kippenberg T J and Vahala K J 2008 *Science* **321** 1172
[6] Xiong H, Si L G, Lü X Y, Yang X X and Wu Y 2015 *Sci. China Phys. Mech. Astron.* **58** 1
[7] Sun C P and Li Y 2015 *Sci. China Phys. Mech. Astron.* **58** 1

[8] Kani A, Sarma B and Twamley J 2022 *Phys. Rev. Lett.* **128** 013602
[9] Xiang Z L, Ashhab S, You J Q and Nori F 2013 *Rev. Mod. Phys.* **85** 623
[10] Kurizki G, Bertet P, Kubo Y, Molmer K, Petrosyan D, Rabl P and Schmiedmayer J 2015 *Proc. Natl. Acad. Sci. USA* **112** 3866
[11] Haroche S and Raimond J M 2006 *Exploring the Quantum* (Oxford Graduate Texts, Oxford)
[12] Walther H, Varcoe B T, Englert B G and Becker T 2006 *Rep. Prog. Phys.* **69** 1325
[13] LaHaye M D, Suh J, Echternach P M, Schwab K C and Roukes M L 2009 *Nature* **459** 960
[14] O'Connell A D, Hofheinz M, Ansmann M, Bialczak R C, Lenander M, Lucero E, Neeley M, Sank D, Wang H, Weides M, Wenner J, Martinis J M and Cleland A N 2010 *Nature* **464** 697
[15] Li P B, Zhou Y, Gao W B and Nori F 2020 *Phys. Rev. Lett.* **125** 153602
[16] Restrepo J, Ciuti C and Favero I 2014 *Phys. Rev. Lett.* **112** 013601
[17] Sete E A and Eleuch H 2014 *Phys. Rev. A* **89** 013841
[18] Wang H, Gu X, Liu Y, Miranowicz A and Nori F 2014 *Phys. Rev. A* **90** 023817
[19] Holz T, Betzholz R and Bienert M 2015 *Phys. Rev. A* **92** 043822
[20] Černotík O and Hammerer K 2016 *Phys. Rev. A* **94** 012340
[21] Genes C, Vitali D and Tombesi P 2008 *Phys. Rev. A* **77** 050307
[22] Genes C, Ritsch H, Drewsen M and Dantan A 2011 *Phys. Rev. A* **84** 051801
[23] Dantan A, Nair B, Pupillo G and Genes C 2014 *Phys. Rev. A* **90** 033820
[24] Carmele A, Vogell B, Stannigel K and Zoller P 2014 *New J. Phys.* **16** 063042
[25] Nie W, Chen A, Lan Y, Liao Q and Zhu S 2016 *J. Phys. B: At. Mol. Opt. Phys.* **49** 025501
[26] Hei X L, Li P B, Pan X F and Nori F 2023 *Phys. Rev. Lett.* **130** 073602
[27] Restrepo J, Favero I and Ciuti C 2017 *Phys. Rev. A* **95** 023832
[28] Zou F, Fan L B, Huang J F and Liao J Q 2019 *Phys. Rev. A* **99** 043837
[29] Liao J Q, Huang J F, Tian L, Kuang L M and Sun C P 2020 *Phys. Rev. A* **101** 063802
[30] Wang Y M, Zhang G Q and You W L 2018 *Laser Phys. Lett.* **15** 105201
[31] Yang J Y, Yang Z, Zhao C S, Peng R, Chao S L and Zhou L 2021 *Opt. Express* **29** 36167
[32] Bhattacharya M, Uys H and Meystre P 2008 *Phys. Rev. A* **77** 033819
[33] Thompson J D, Zwickl B M, Jayich A M, Marquardt F, Girvin S M and Harris J G E 2008 *Nature* **452** 72
[34] Sankey J C, Yang C, Zwickl B M, Jayich A M and Harris J G E 2010 *Nat. Phys.* **6** 707
[35] Li G, Nie W, Li X, Li M, Chen A and Lan Y 2019 *Sci. China Phys. Mech. Astron.* **62** 100311
[36] Bowen W P and Milburn G J 2015 *Quantum Optomechanics* (CRC Press)
[37] Xuereb A, Barbieri M and Paternostro M 2012 *Phys. Rev. A* **86** 013809
[38] Yang X H, Ling Y, Shao X P and Xiao M 2017 *Phys. Rev. A* **95** 052303
[39] Wang Y D, Chesi S and Clerk A A 2015 *Phys. Rev. A* **91** 013807
[40] Jiang C, Tserkis S, Collins K, Onoe S, Li Y and Tian L 2020 *Phys. Rev. A* **101** 042320
[41] Xiang Y, Sun F X, Wang M, Gong Q H and He Q Y 2015 *Opt. Express* **23** 30104
[42] Li J, Zhu S Y and Agarwal G S 2018 *Phys. Rev. Lett.* **121** 203601
[43] Thompson J D, Zwickl B M, Jayich A M, Marquardt F, Girvin S M and Harris J G E 2008 *Nature* **452** 72
[44] Jaynes E T and Cummings F W 1963 *Proc. IEEE* **51** 89
[45] See Appendix for more details.
[46] Allen L and Eberly J H 1975 *Optical Resonance and Two-level Atoms* (New York: Wiley)
[47] Sankey J C, Yang C, Zwickl B M, *et al.* 2010 *Nat. Phys.* **6** 707
[48] Lü X Y, Zheng L L, Zhu G L and Wu Y 2018 *Phys. Rev. Appl.* **9** 064006
[49] Zhang Z C and Wang X G 2020 *Opt. Express* **28** 2732
[50] Polkovnikov A, Sengupta K, Silva A, *et al.* 2011 *Rev. Mod. Phys.* **83** 863
[51] Sabiín C and García-Alcaine G 2008 *Eur. Phys. J. D* **48** 435
[52] Roukes M 2001 *Phys. World* **14** 25
[53] Stannigel K, Rabl P, Sørensen A S, Zoller P and Lukin M D 2010 *Phys. Rev. Lett.* **105** 220501
[54] Heinrich G, Ludwig M, Qian J, Kubala B and Marquardt F 2011 *Phys. Rev. Lett.* **107** 043603
[55] Lassen M, Delaubert V, Janousek J, Wagner K, Bachor H A, Lam P K, Treps N, Buchhave P, Fabre C and Harb C C 2007 *Phys. Rev. Lett.* **98** 083602
[56] Massel F, Heikkilä T T, Pirkkalainen J M, Cho S U, Saloniemi H, Hakonen P J and Sillanpää M A 2011 *Nature* **480** 351
[57] Xu X W, Zhao Y J and Liu Y X 2013 *Phys. Rev. A* **88** 022325
[58] Seok H, Buchmann L F, Singh S and Meystre P 2012 *Phys. Rev. A* **86** 063829
[59] Ludwig M and Marquardt F 2013 *Phys. Rev. Lett.* **111** 073603
[60] Ludwig M, Hammerer K and Marquardt F 2010 *Phys. Rev. A* **82** 012333
[61] Xuereb A, Genes C and Dantan A 2013 *Phys. Rev. A* **88** 053803
[62] Tomadin A, Diehl S, Lukin M D, Rabl P and Zoller P 2012 *Phys. Rev. A* **86** 033821
[63] Eberle T, Steinlechner S, Bauchrowitz J, Handchen V, Vahlbruch H, Mehmet M, Muller-Ebhardt H and Schnabel R 2010 *Phys. Rev. Lett.* **104** 251102
[64] Khalili F Y and Braginski V 1995 *Quantum Measurement* (Cambridge: Cambridge University)
[65] Hoff U B, Harris G I, Madsen L S, Kerdoncuff H, Lassen M, Nielsen B M, Bowen W P and Andersen U L 2013 *Opt. Lett.* **38** 1413
[66] Taylor M A, Janousek J, Daria V, Knittel J, Hage B, Bachor H A and Bowen W P 2013 *Nat. Photonics* **7** 229
[67] Sete E A and Eleuch H 2010 *Phys. Rev. A* **82** 043810
[68] Zhang Z C, Wang Y P, Yu Y F and Zhang Z M 2018 *Opt. Express* **26** 11915
[69] Purdy T P, Brooks D W C, Botter T, Brahms N, Ma Z Y and Stamper-Kurn D M 2010 *Phys. Rev. Lett.* **105** 133602
[70] Bullier N P, Pontin A and Barker P F 2021 *Phys. Rev. Research* **3** L032022
[71] Thompson J D, Zwickl B M, Jayich A M, Marquardt F, Girvin S M and Harris J G E 2008 *Nature* **452** 72
[72] Thompson J D, Zwickl B M, Jayich A M, Marquardt F, Girvin S M and Harris J G E 2008 *Nature* **452** 72
[73] Sankey J C, Yang C, Zwickl B M, Jayich A M and Harris J G E 2010 *Nat. Phys.* **6** 707
[74] Flowers-Jacobs N E, Hoch S W, Sankey J C, Kashkanova A, Jayich A M, Deutsch C, Reichel J and Harris J G E 2012 *Appl. Phys. Lett.* **101** 221109
[75] Li H K, Liu Y C, Yi X, Zou C L, Ren X X and Xiao Y F 2012 *Phys. Rev. A* **85** 053832
[76] Zhang J S, Li M C and Chen A X 2019 *Phys. Rev. A* **99** 013843
[77] Ma J L, Li Q and Tan L 2021 *Eur. Phys. J. D* **75** 262